

## NIOBIUM- AND PLATINUM-RICH REFRACTORY METAL ALLOYS FROM A TYPE B CAI.

D. Harries<sup>1</sup>, D. Schwander<sup>2</sup>, H. Palme<sup>3</sup> and F. Langenhorst<sup>1</sup>. <sup>1</sup>Institut für Geowissenschaften, Friedrich-Schiller-Universität, Carl-Zeiss-Promenade 10, D-07745 Jena, Germany (dennis.harries@uni-jena.de), <sup>2</sup>Institut für Physik, Johannes Gutenberg-Universität, Staudingerweg 7, D-55128 Mainz, Germany, <sup>3</sup>Forschungsinstitut und Naturkundemuseum Senckenberg, Senckenberganlage 25, D-60325 Frankfurt am Main, Germany.

**Introduction:** Refractory metal nuggets (RMNs) found in carbonaceous chondrites are nm- to  $\mu\text{m}$ -sized particles of metallic alloys consisting of Os, Ru, Ir, Pt, Mo, W, Fe, and subordinate amounts of other elements. The common property of the components of RMNs are low vapor pressures and, hence, high condensation-sublimation temperatures of the elements in the metallic state, suggesting, that RMNs are possible nebular condensates [1]. For example, the siderophile elements Au and Pd have calculated condensation temperatures less than that of metallic Fe and are not found in significant quantities in RMNs, while W and Pt, having similar solar abundances but higher condensation temperatures, are frequently found.

RMNs are monophase alloys [2] and distinguished from alteration-related ‘opaque assemblages’ (OAs), which consist of multiple alloys associated with oxidized compounds like  $\text{Ca}(\text{W},\text{Mo})\text{O}_4$  (scheelite-powellite) and  $\text{MoS}_2$  (molybdenite).

In order to better understand the mechanisms of formation of RMNs we have conducted a detailed study of RMNs found *in situ* within a CAI using analytical transmission electron microscopy (TEM) and focused ion beam (FIB) assisted sample extraction.

**Material:** The sample studied is a polished fragment of the Allende Type B CAI A39. The CAI consists of abundant melilite and fassaite, forming millimeter-sized, interlocking grains. Poikilitically enclosed within these are numerous, euhedral to subhedral spinel grains. Sub-micrometer-sized RMNs and OAs occur scattered within these three minerals.

**Results:** Currently, we have extracted and studied a total of seven RMNs from the A39 CAI.

**Chemical compositions.** The RMNs analyzed by TEM-EDX show an average composition of approximately  $\text{Ru}_{29}\text{Pt}_{19}\text{Mo}_{18}\text{Os}_{10}\text{Ir}_{10}\text{Nb}_4\text{Fe}_4\text{Ni}_2\text{Rh}_2\text{W}_1$ . Pt contents range between  $\sim 14$  and  $24$  at%. Most notably, four of the seven RMNs contain considerable amounts of Nb, ranging from  $\sim 2$  to  $12$  at%.

**Crystallography.** Selected area electron diffraction (SAED) patterns obtained from individual RMNs show that all RMNs sampled have hexagonal structures, similar to those found in Murchison residues [1, 2]. The average lattice constants  $a \approx 0.273$  nm and  $c \approx 0.445$  nm are indistinguishable from those of the Murchison RMNs.

**Physical properties and mineral associations.** The sizes of the RMNs sampled range from  $260$  nm to just more than  $3$   $\mu\text{m}$ . All except one are single crystals. The polycrystalline one is associated with a Ca-Nb-O phase and more likely an OA than a RMN.

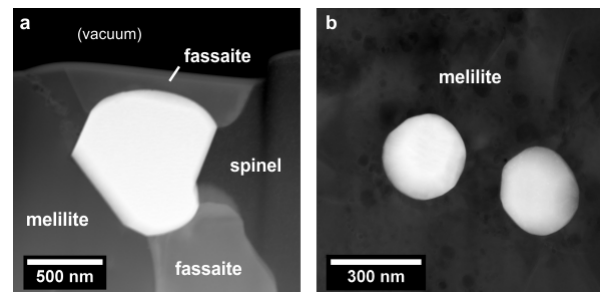


**Figure 1.** DF-STEM images of FIB-extracted RMNs. (a) RMN5 in boundary clinopyroxene. (b) RMN9a and 9b in melilite.

RMN5 (Fig. 1a) is a  $\sim 1$   $\mu\text{m}$  large grain found partially enclosed in so-called ‘boundary clinopyroxene’, which is fassaite fully or partially covering the surfaces of spinel grains within melilite of Type B CAIs [3,4]. Figure 1 shows that the RMN is situated on a protrusion of the spinel grain, which, therefore, appears to be embayed or corroded with respect to the fassaite rim. This observation suggests that the attachment of the RMN to the spinel surface predates the formation of the fassaite rims, which apparently consumed parts of the spinel. Moreover, at the interface to the spinel, the RMN shows a reentrant angle, strongly suggesting that the original spinel surface and the RMN formed contemporaneously. Interestingly, the enclosed RMN shows rounded interfaces toward the fassaite, while the interfaces are straight toward the melilite and spinel. This suggests that the fassaite may be the youngest phase and that during its formation the RMN interface recrystallized to attain a minimum interface energy.

RMN9 (Fig. 1b) was found to consist of two separate grains of almost identical sizes ( $\sim 260$  nm) and shapes ( $\pm$ spherical) in close proximity ( $\sim 400$  nm from center to center). The two grains are completely surrounded by melilite. Compositionally, the two grains are clearly distinct, showing differences of 3-5 at% in Ru, Os, Ir, and Pt. Because of the nearly identical sizes, the compositional differences suggest that the two

RMNs did not form in the close proximity in which they have been found.

**Discussion:** Boundary clinopyroxene in Type B CAIs has been interpreted to be a relict condensate [3] or, alternatively, a reaction product during partial melting of CAIs [4]. Either way, the replacement of the spinel seems to require the involvement of a mobile phase (gas or melt) due to mass balance constraints. If the spinel and its fassaite rims are indeed relict condensates having survived the melting of the CAI, then RMN5 must be a condensate as well. However, because the fassaite rim appears to be the youngest feature, it seems rather likely that the boundary clinopyroxene formed through an in situ reaction along the spinel-melilite interface. In this case the RMN could have grown on the spinel surface as a condensate or during precipitation from the CAI melt.

*Compositions vs. condensation models.* The Pt and Nb-rich compositions of the A39 RMNs are distinct from those of the RMNs studied by [1,2] and do not match well with the condensation model of [2]. Particularly, Pt exceeds the calculated contents by a factor of about 2-3. We have performed condensation calculations (Fig. 2) including additional elements and the effect of  $f_{O_2}$  on the gas phase species.

For a cooling path along  $\log(f_{O_2}) = IW-7$  ( $IW =$  iron-wüstite-buffer), close to the  $f_{O_2}$  of a solar gas, the calculations indicate small amounts of Nb and V to be present in the metal phase (for unity activity coefficients and no other V- and Nb-bearing phases present). Zr and Ti are present as  $ZrO_{(g)}$  and  $TiO_{(g)}$  species in the gas and do not condense into the metal (Ta has too a low abundance to be relevant). At lower  $f_{O_2}$ , the amount of Nb in the metal increases due to a higher fraction of  $Nb_{(g)}$  relative to  $NbO_{(g)}$  in the gas phase. Because Zr and Nb are expected to have activity coefficients  $< 1$  in noble metal alloys due to the Engel-Brewer correlation [5], it seems possible that significant amounts of Nb could condense into RMNs even if Nb-bearing perovskite condenses at the same time.

The high Pt content cannot be reconciled with condensation from a solar gas at any reasonable  $f_{O_2}$  if only a single phase condenses. Because Pt is only slightly less volatile than Fe, it is effectively diluted by condensing Fe. Highly oxidizing conditions, hindering metallic Fe to condense, would fully oxidize Nb. The only way to obtain compositions similar to the observed ones would be the condensation of Fe, Ni, Cr, and V into separate phases, in which Pt is incompatible, or a significant depletion of the gas relative to the solar abundances for these elements (Fig. 2c).

Unless reasonable mechanisms for the above fractionations can be found, the secondary modification of

the metal compositions during CAI melting must be considered as well. However, also in this case a mechanism must be found which can fractionate Pt into the hexagonal alloys without diluting it with Fe or oxidizing Nb.

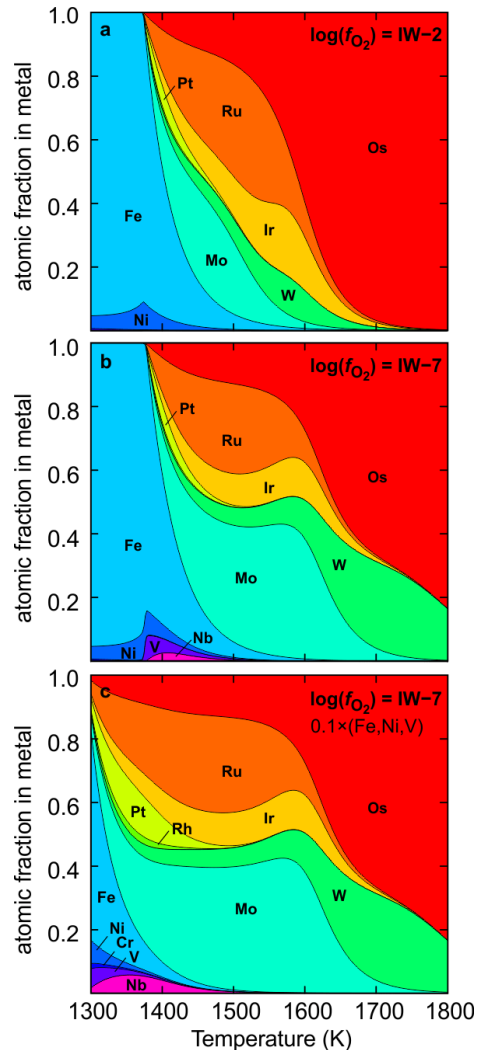


**Figure 2.** Condensation calculations ( $P_{tot} = 0.0001$  bar) for the system Os, Ru, Ir, Pt, Rh, Pd, W, Mo, Fe, Ni, Cr, V, Zr, Nb, Ti. For the latter nine elements, the fractions of the  $MO_{(g)}$  gaseous oxide species were calculated as a function of  $f_{O_2}$ . No co-condensing phases were considered. In (c), the abundances of Fe, Ni, and V were lowered by a factor of 10 relative to the solar abundances in the former plots.

**References:** [1] Berg T. et al. (2009) *ApJ*, 702, L172–L176. [2] Harries D. et al. (2012) *Meteoritics & Planet. Sci.*, in press. [3] Kuehner S. M. et al. (1989) *GRL*, 16, 775–778. [4] Paque J. M. (2009) *Meteoritics & Planet. Sci.*, 44, 665–687. [5] Fegley B. Jr. and Kornacki A. S. (1987) *EPSL*, 68, 181–197.

This study was supported by DFG grant LA 830/14-1.